

Supporting Information for

Spectrally Separated Dual Functional Fluorescent Nanosensors for Subcellular Lysosomal Detection of Hypochlorous Acid and Chloride

Yunxin Cui^{#a}, Jianhong Wu^{#b}, Jingying Zhai^b, Yifu Wang^a, and Xiaojiang Xie^{*a}

a. Department of Chemistry, Southern University of Science and Technology, Shenzhen, 518055, China.

b. Academy for Advanced Interdisciplinary Studies, Southern University of Science and Technology, Shenzhen, 518055, China.

* Corresponding author E-mail: xiexj@sustech.edu.cn

equal contribution

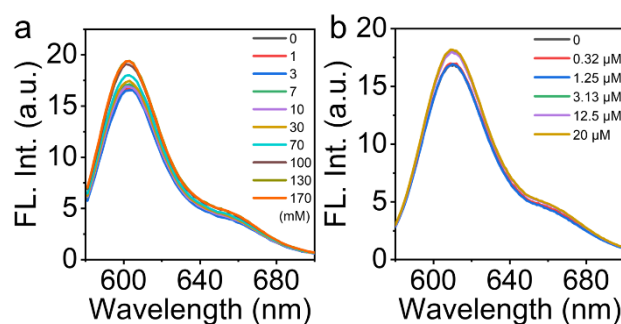


Fig. S1 (a) Fluorescence emission spectra of the nanosensors with different concentrations of Cl^- . (b) Fluorescence emission spectra of the nanosensors with different concentrations of HClO . The nanosensors contained only LRed. Excitation: 561 nm.

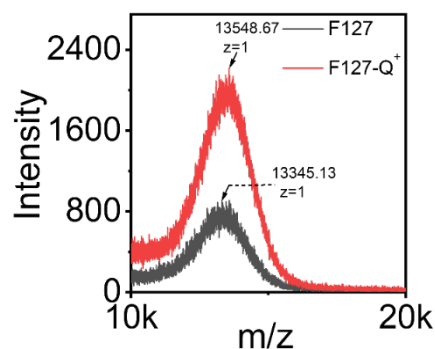


Fig. S2 Comparison of the MALDI-TOF spectra of F127 and F127-Q⁺.

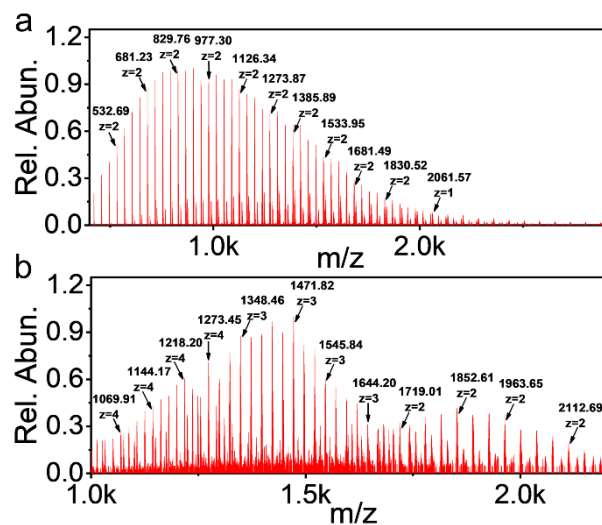


Fig. S3 (a) Electrospray ionization mass spectroscopic (ESI-MS) characterization of PDMS-NH₂. (b) ESI-MS characterization of PDMS-Cy5.

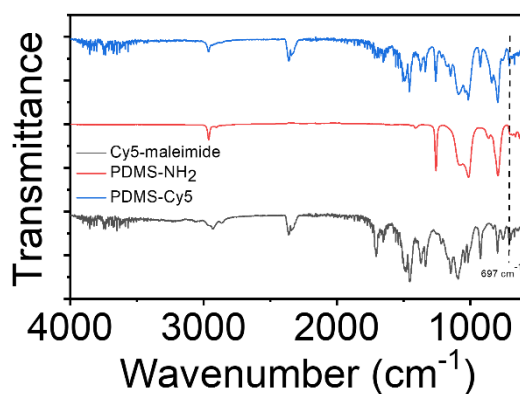


Fig. S4 Comparison of the Fourier transform infrared (FT-IR) spectra of Cy5-maleimide, PDMS-NH₂ and PDMS-Cy5. The dashed line marks the transmittance (a.u.) at 697 cm⁻¹, corresponding to the bending of the C-H bond on the maleic amide group before Michael addition.

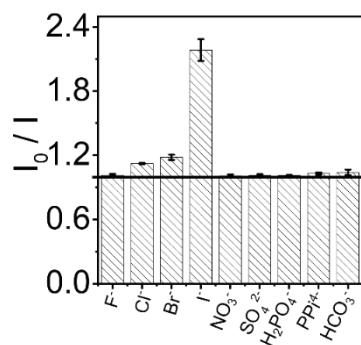


Fig. S5 Fluorescence response of NS_Cl&HClO under different anions (1 mM) based on the emission of F127-Q⁺ at 448 nm. I_0 represent the initial emission intensity without the addition of the anions. Excitation: 365 nm.

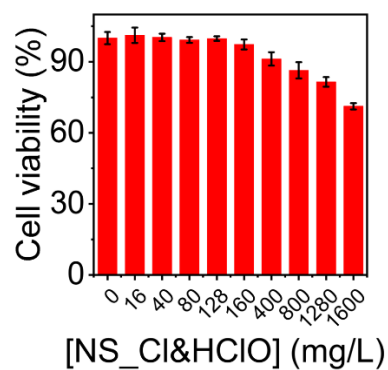


Fig. S6 Cell viability under incubation with NS_Cl&HClO of different mass concentration. Evaluated with the Commercial CCK-8 assay.

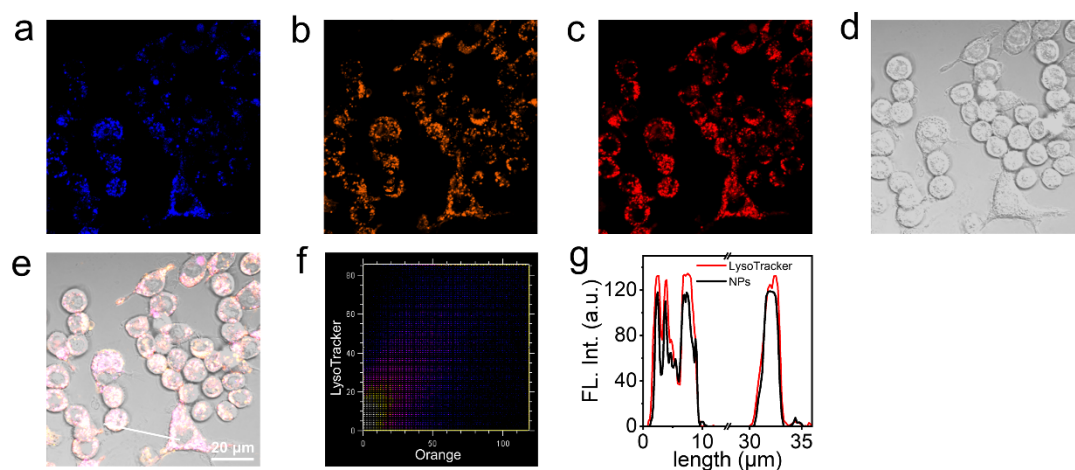


Fig. S7 Colocalization of NS_Cl&HCIO and LysoTracker Deep Red in RAW264.7 cells. (a) The fluorescence emission of the Cl⁻ sensitive Q⁺ from NS_Cl&HCIO. (b) The emission of LRed from NS_Cl&HCIO. (c) The emission from LysoTracker Deep Red. (d) Bright field. (e) Merge of (a), (b), (c) and (d). (f) Correlation scatter plot of LRed from NS_Cl&HCIO and LysoTracker Deep Red. (g) The intensity profile along the line marked in (e). Note that to avoid bias, Cy5 was removed from the nanosensors because of the emission overlap with LysoTracker Deep Red. Signals in the Blue, Orange, and Red channels were respectively collected from 410-530 nm, 570-630 nm, and 650-700 nm with respective excitation at 405, 561, and 640 nm.

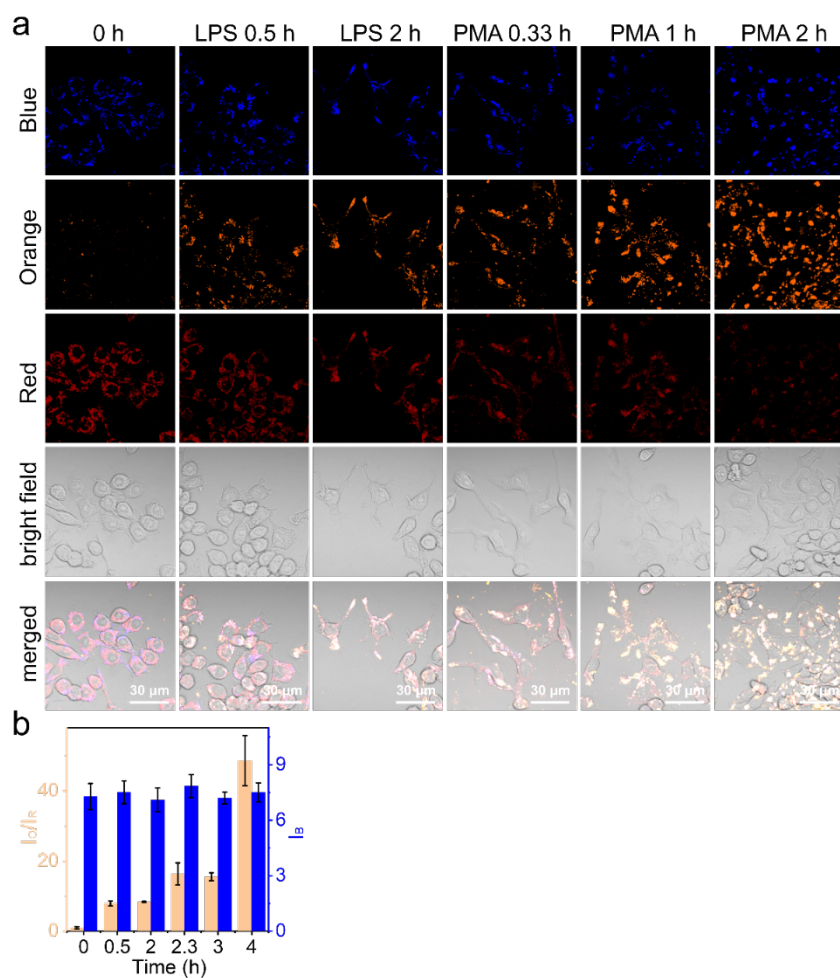


Fig. S8 (a) Time-lapse CLSM imaging of NS_Cl&HClO-labelled RAW264.7 under successive incubation with 7 $\mu\text{g/mL}$ of LPS and then 3 $\mu\text{g/mL}$ of PMA. (b) The column graph showing the dynamics of lysosomal signals based on the intensity ratio between the Orange and Red channels (I_{O/I_R}) and the intensity of the Blue channel (I_B) during LPS and PMA stimulation. Signals in the Blue, Orange, and Red channels were respectively collected from 410-530 nm, 570-630 nm, and 650-700 nm with respective excitation at 405, 561, and 640 nm.

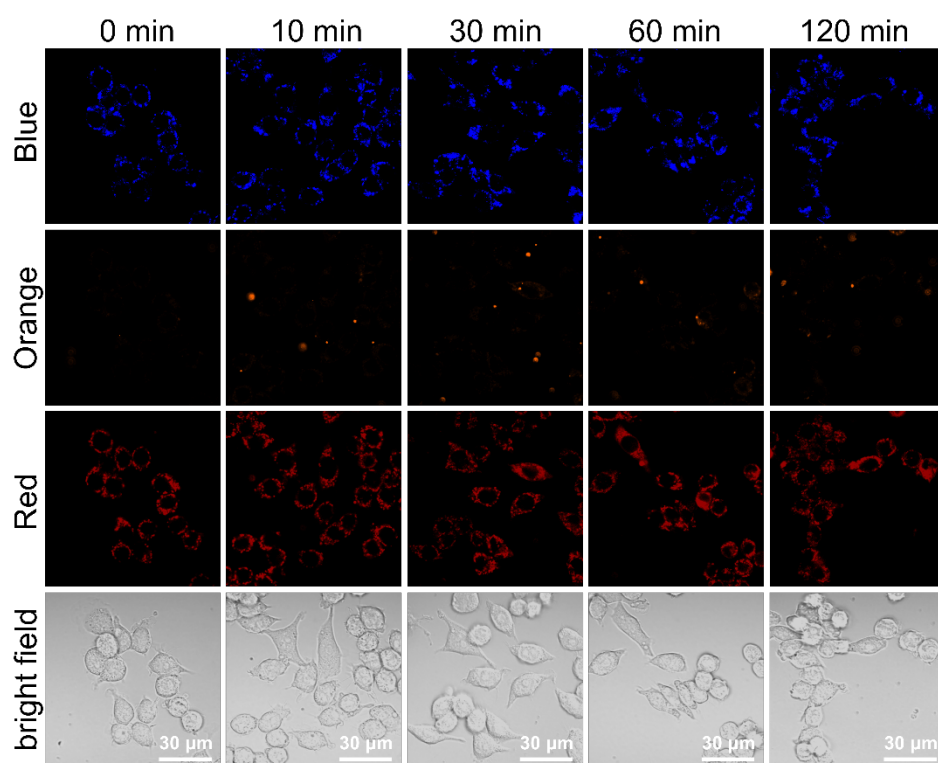


Fig. S9 Time-lapse CLSM imaging of NS_Cl&HClO-labelled RAW264.7 incubated with 200 nM of Bafilomycin A1. Signals in the Blue, Orange, and Red channels were respectively collected from 410-530 nm, 570-630 nm, and 650-700 nm with respective excitation at 405, 561, and 640 nm.

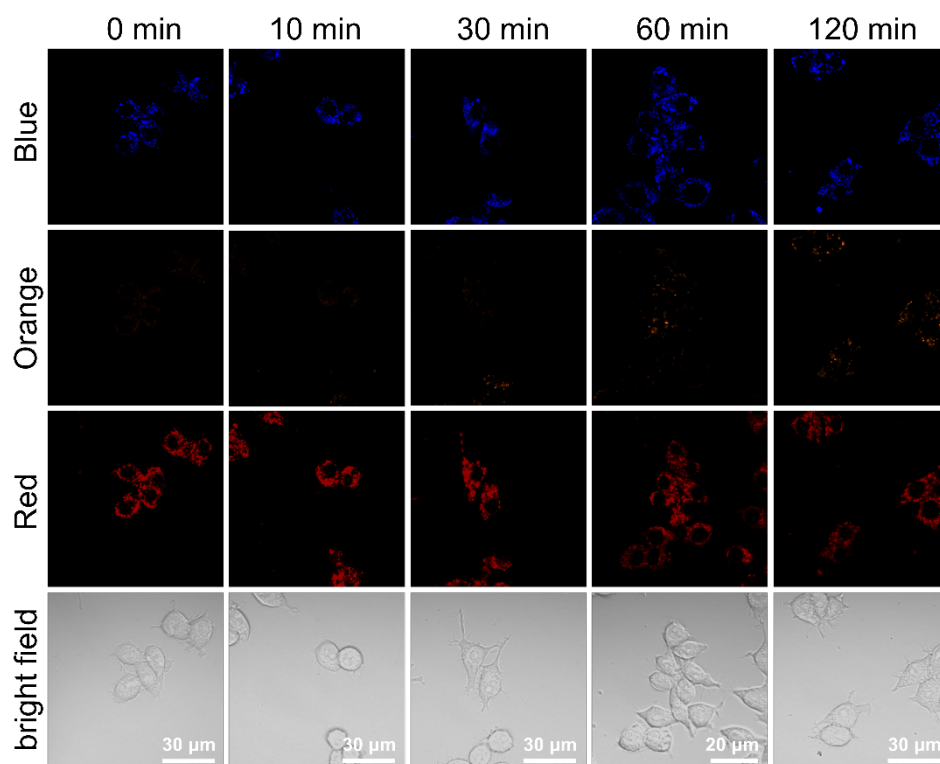


Fig. S10 Time-lapse CLSM imaging of NS_Cl&HClO-labelled RAW264.7 incubated with 100 μ M of ABAH. Signals in the Blue, Orange, and Red channels were respectively collected from 410-530 nm, 570-630 nm, and 650-700 nm with respectively excitation at 405, 561, and 640 nm.

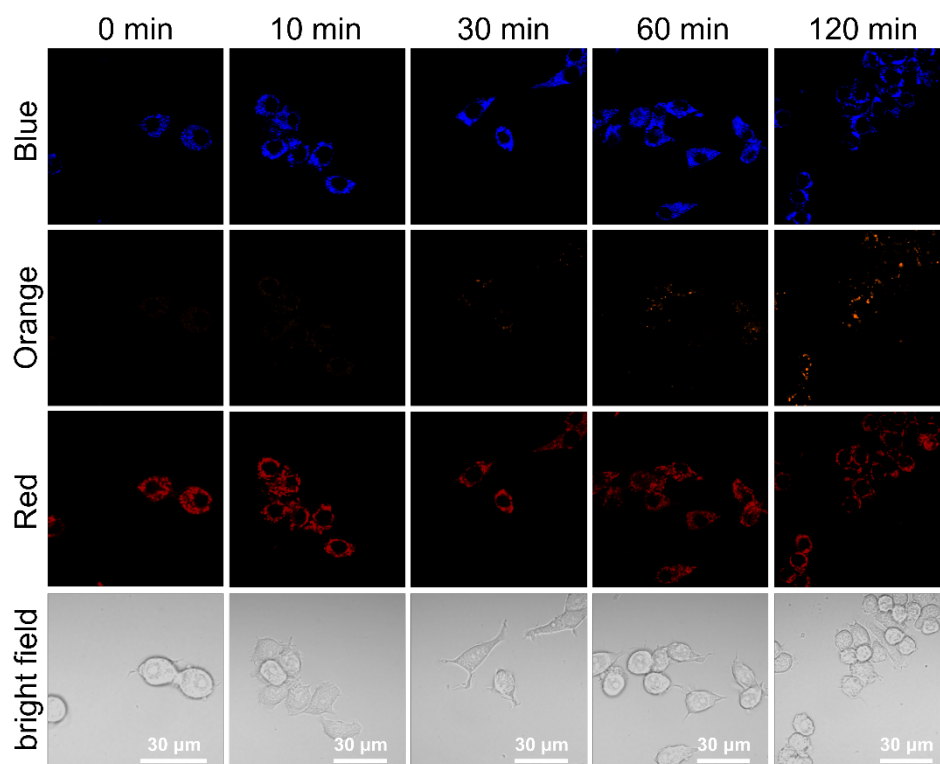


Fig. S11 Time-lapse CLSM imaging of NS_Cl&HClO-labelled RAW264.7 incubated with 100 μ M of NPPB. Signals in the Blue, Orange, and Red channels were respectively collected from 410-530 nm, 570-630 nm, and 650-700 nm with respectively excitation at 405, 561, and 640 nm.